Original Article

Construction of a TFs-miRNA-mRNA network related to idiopathic pulmonary fibrosis

Minhong Su[1#^], Junfang Liu[1#^], Xiping Wu[1^], Xin Chen[1^], Qiang Xiao[2], Ning Jiang[3^]

[1]Department of Respiratory and Critical Care Medicine, Zhujiang Hospital, Southern Medical University, Guangzhou, China; [2]Department of Pulmonary and Critical Care Medicine, Shunde Hospital, Southern Medical University, Foshan, China; [3]Department of Urology, Zhujiang Hospital, Southern Medical University, Guangzhou, China

Contributions: (I) Conception and design: N Jiang, Q Xiao; (II) Administrative support: N Jiang; (III) Provision of study materials or patients: Q Xiao; (IV) Collection and assembly of data: J Liu, X Wu, X Chen; (V) Data analysis and interpretation: M Su, N Jiang; (VI) Manuscript writing: All authors; (VII) Final approval of manuscript: All authors.

[#]These authors contributed equally to this work and should be considered as co-first authors.

Correspondence to: Qiang Xiao. Department of Pulmonary and Critical Care Medicine, Shunde Hospital, Southern Medical University, 1 Jiazi Road, Licun, Lunjiao Street, Shunde District, Foshan 528300, China. Email: xiaoqiang@smu.edu.cn; Ning Jiang. Department of Urology, Zhujiang Hospital, Southern Medical University, 253 Gongye Middle Avenue, Haizhu District, Guangzhou 510280, China. Email: jiangn6@foxmail.com.

Background: The transcription factors (TFs)-microRNA (miRNA)-messenger RNA (mRNA) network plays an important role in a variety of diseases. However, the relationship between the TFs-miRNA-mRNA network and idiopathic pulmonary fibrosis (IPF) remains unclear.

Methods: The GSE110147 and GSE53845 datasets from the Gene Expression Omnibus (GEO) database were used to process differentially expressed genes (DEGs) analysis, gene set enrichment analysis (GSEA), weighted gene co-expression network analysis (WGCNA), as well as Gene ontology and Kyoto Encyclopedia of Genes and Genomes (KEGG) analyses. The GSE13316 dataset was used to perform differentially expressed miRNAs (DEMs) analysis and TFs prediction. Finally, a TFs-miRNA-mRNA network related to IPF was constructed, and its function was evaluated by Gene Ontology (GO) and KEGG analyses. Also, 19 TFs in the network were verified by quantitative real time polymerase chain reaction (qRT-PCR).

Results: Through our analysis, 53 DEMs and 2,630 DEGs were screened. The GSEA results suggested these genes were mainly related to protein digestion and absorption. The WGCNA results showed that these DEGs were divided into eight modules, and the GO and KEGG analyses results of blue module genes showed that these 86 blue module genes were mainly enriched in cilium assembly and cilium organization. Moreover, a TFs-miRNA-mRNA network comprising 25 TFs, 11 miRNAs, and 60 mRNAs was constructed. Ultimately, the functional enrichment analysis showed that the TFs-miRNA-mRNA network was mainly related to the cell cycle and the phosphatidylinositol 3 kinase-protein kinase B (*PI3K-Akt*) signaling pathway. Furthermore, experimental verification of the TFs showed that *ARNTL*, *TRIM28*, *EZH2*, *BCOR*, and *ASXL1* were sufficiently up-regulated in the transforming growth factor (TGF)-β1 treatment groups, while *BCL6*, *BHLHE40*, *FOXA1*, and *EGR1* were significantly down-regulated.

Conclusions: The novel TFs-miRNA-mRNA network that we constructed could provide new insights into the underlying molecular mechanisms of IPF. *ARNTL*, *TRIM28*, *EZH2*, *BCOR*, *ASXL1*, *BCL6*, *BHLHE40*, *FOXA1*, and *EGR1* may play important roles in IPF and become effective biomarkers for diagnosis and treatment.

Keywords: Idiopathic pulmonary fibrosis (IPF); transcription factors (TFs); network; weighted gene co-expression network analysis (WGCNA); biomarker

^ ORCID: Minhong Su, 0000-0002-3933-2534; Junfang Liu, 0000-0002-0839-2323; Xiping Wu, 0000-0003-1822-1664; Xin Chen, 0000-0002-1920-8835; Ning Jiang, 0000-0002-2829-2565.

Submitted Nov 22, 2022. Accepted for publication Jan 07, 2023. Published online Jan 31, 2023.
doi: 10.21037/atm-22-6161
View this article at: https://dx.doi.org/10.21037/atm-22-6161

Introduction

Idiopathic pulmonary fibrosis (IPF), the most common idiopathic interstitial pneumonia, is a chronic progressive fibrotic lung disease of unknown etiology that occurs predominantly in elderly adults, with a median age at diagnosis of 65 years old (1). It is associated with a high mortality rate, and therapies that slow disease progression are now available (2). Overall, patients with IPF have a similar life expectancy to those with non-small cell lung cancer, with a reported median survival rate estimate of 50% at 3 years and 20% at 5 years post-diagnosis (3,4). In recent years, the prevalence of IPF and the rates of hospital admissions and deaths due to the disease appear to be increasing, suggesting an increasing disease burden (5-7). Therefore, there is an urgent need to further understand the pathogenesis of IPF and identify novel markers to provide new research ideas for clinical treatment.

Historically, IPF was considered a chronic inflammatory disease, which gradually progresses to fibrosis. However, this concept was reassessed following the recognition that anti-inflammatory treatment did not improve disease outcomes, and the immunosuppressive treatment strategy of prednisolone and azathioprine was shown to increase mortality (8,9). Currently, IPF is generally considered to be the result of the interaction of multiple genetic and environmental risk factors that repeatedly act on the local alveolar epithelium to cause micro-injury. These micro-injuries trigger aberrant epithelial-fibroblast communication, induce myofibroblast activation, and cause massive extracellular matrix deposition and interstitial remodeling (10).

In recent years, microRNA (miRNA) has gained increasing attention from researchers in the field of IPF. Several reports have revealed the critical roles of miRNA and targeted messenger RNA (mRNA) in the development of various diseases, including IPF. Moreover, the expression of target genes could also be regulated by transcription factors (TFs) combining cis-elements at promoter locations (11). It is known that some TFs are involved in the pathogenesis of IPF. For example, early growth response transcription factors were found to be key mediators of fibrosis (12). Moreover, epithelial-mesenchymal transition (EMT) is known as an important feature in IPF and it is regulated by several TFs, which are members of prominent families of master regulators of transcription, such as the Forkhead family (*FOXO*), Twist family (*TWIST*), *SNAIL* family of zinc-finger transcription factors (*SNAIL*) and zinc-finger E-box-binding family (*ZEB*) (13). Thus, TFs may play important roles in the development of IPF. Many studies showed that transforming growth factor-β1 (TGF-β1) plays a central role in the development of IPF (14). TGF-β1 promotes the fibrotic process of IPF through a variety of signaling pathways, including the MAPK, Smad and ERK signaling pathways (15-18). For example, transforming growth factor (TGF)-β induces *SMAD* family member 3 (*SMAD3*), which inhibits *let-7d* expression by binding to the upstream region of *let-7* (19). The down-regulated expression of *let-7* and consequent over-expression of high mobility group AT-hook 2 (*HMGA2*) decreases the expression of epithelial markers, cytokeratin and tight junction protein 1 (*TJP1*), and increases the expression of mesenchymal markers, actin alpha 2 (*ACTA2*) and vimentin (*VIM*), thereby inducing EMT to promote pulmonary fibrosis (20,21). Liu *et al.* demonstrated that *TGF-β* signaling leads to significant overexpression of *microRNA-21* (*miR-21*) in the lungs of bleomycin-induced mice, which acts as an amplifying circuit to increase the fibrotic activity of *TGF-β* (22). Yang *et al.* showed that *miR-200* family

Highlight box

Key findings

- We construct a TFs-miRNA-mRNA network related to IPF and verify TFs by qRT-PCR.

What is known and what is new?

- Many transcription factors (TFs), microRNAs and mRNAs play important roles in IPF.
- We construct a TFs-miRNA-mRNA network related to IPF and perform functional enrichment analysis.

What is the implication, and what should change now?

- The novel TFs-miRNA-mRNA network provide new insights into the underlying molecular mechanisms of IPF.
- *ARNTL*, *TRIM28*, *EZH2*, *BCOR*, *ASXL1*, *BCL6*, *BHLHE40*, *FOXA1*, and *EGR1* may become effective biomarkers for diagnosis and treatment of IPF.

members (200a, 200b, 200c) inhibit EMT and reverse the fibrotic function of lung fibroblasts (23). Yang *et al.* also showed that *miR-200* family members act as negative regulators of *TGF-β*-mediated pulmonary fibrosis, attenuate the expression of *TGF-β*-mediated mesenchymal markers, and can be candidates for the treatment of pulmonary fibrosis (23). Zhu *et al.* constructed a miRNA-mRNA network in IPF (24), but the reason for differential mRNAs and miRNAs was not explored. We conjectured that with so many differentially expressed mRNAs and miRNAs in IPF, it is likely that broad-spectrum regulatory factors such as TFs are involved upstream. Therefore, we predicted the possible regulatory causes of mRNA and miRNA differential expression by constructing a TFs-miRNA-mRNA regulatory network, thus facilitating further research exploration in the future. In addition, in the current study, the approach of using WGCNA can better focus on the most important gene modules within IPF tissue samples and provide more accurate and reliable downstream genes to build the network compared with simple differential gene intersection. Therefore, constructing the TFs-miRNA-mRNA regulatory network in IPF is really important and necessary.

In this study, we first screened several differentially expressed miRNAs (DEMs) in the lung tissues of IPF patients and compared these with normal tissues by analyzing the GSE13316 dataset downloaded from the Gene Expression Omnibus (GEO) database. Then, DE-mRNAs [differentially expressed genes (DEGs)] between IPF tissues and normal tissues were obtained using the GSE110147 and GSE53845 datasets downloaded from the GEO database. Gene set enrichment analysis (GSEA) of the DEGs was conducted using the clusterprofiler R package (25). To screen an important module in DEGs, weighted gene co-expression network analysis (WGCNA) analysis of the DEGs was performed using the "WGCNA" R package (26). Subsequently, Gene Ontology (GO) functional annotation and Kyoto Encyclopedia of Genes and Genomes (KEGG) pathway enrichment analysis (27,28) of the important module genes were conducted using the clusterprofiler R package. Next, the miRNA-mRNA network was constructed by using the miRDB, miRTarBase, and TargetScan databases. TFs prediction of the miRNAs in the miRNA-mRNA network was performed using the base of the TransmiR v2.0 database. Finally, a TFs-miRNA-mRNA network contributing to the onset and progression of IPF was successfully established. GO and KEGG analyses of the TFs-miRNA-mRNA network were conducted using the clusterprofiler R package. This study credibly discriminated human IPF-related miRNAs and provided a novel approach to identifying the pathological mechanisms and potential targets of IPF. We present the following article in accordance with the STREGA reporting checklist (available at https://atm.amegroups.com/article/view/10.21037/atm-22-6161/rc).

Methods

Data download

First, we searched the GEO database (https://www.ncbi.nlm.nih.gov/geoprofiles) for datasets related to miRNA and IPF by using the keywords "miRNA" and "idiopathic pulmonary fibrosis". Next, three datasets (GSE13316, GSE110147, and GSE53845) were downloaded. For miRNA expression profiling related to IPF (GSE13316, platform: GPL6955 Agilent-016436 Human miRNA Microarray 1.0), 10 samples were obtained from the surgical remnants of biopsies or lungs explanted from patients with IPF who underwent pulmonary transplant, and 10 control normal lung tissues obtained from the disease-free margins with normal histology of lung cancer resection specimens. The study was conducted in accordance with the Declaration of Helsinki (as revised in 2013).

For mRNA expression profiling in IPF, 22 fresh frozen lung samples were obtained from the recipient's organs of 22 patients with IPF and 11 normal lung tissue (n=11) samples were obtained from the tissue flanking lung cancer resections (GSE110147, GPL6244 Affymetrix Human Gene 1.0 ST Array). In the GSE53845 dataset (platform: GPL6480 Agilent-014850 Whole Human Genome Microarray 4x44K G4112F), RNA was extracted directly from lung tissue samples from 40 IPF patients and eight healthy controls. The workflow of this study is shown in *Figure 1*.

DEMs and DEGs screening

Firstly, the DEMs between the IPF and normal tissues were screened using the GEO2R online software. $P<0.05$ was considered statistically significant. At the same time, the differentially expressed mRNAs between the IPF and normal tissues were also screened by the GEO2R online software. We used the Benjamini & Hochberg (false discovery rate) method to adjust the P values, and an adjusted P value <0.05 was selected as the threshold.

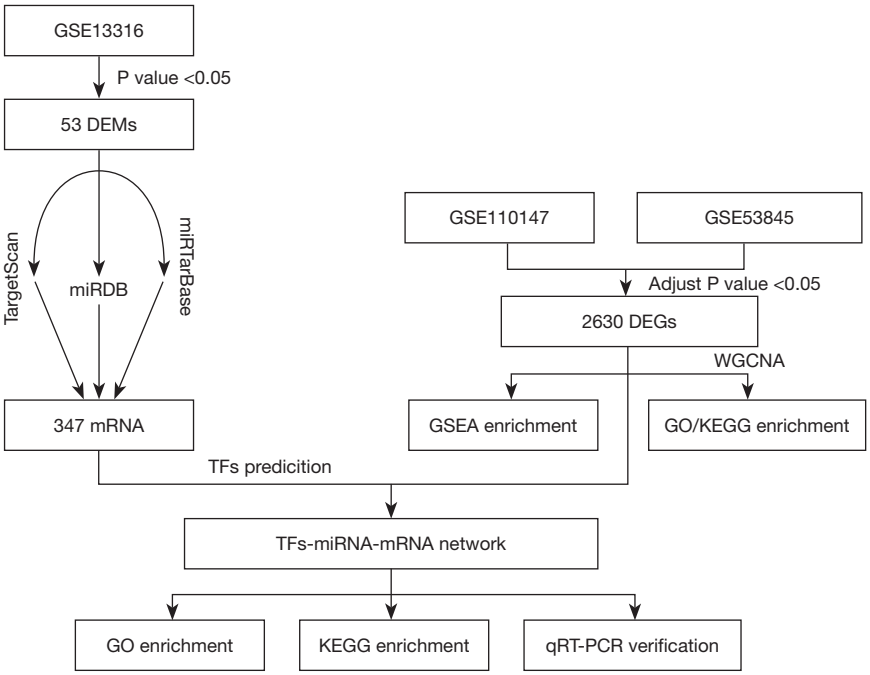

Figure 1 Workflow of this study design. DEM, differentially expressed miRNA; WGCNA, weighted gene co-expression network analysis; GSEA, gene set enrichment analysis; GO, Gene Ontology; KEGG, Kyoto Encyclopedia of Genes and Genomes; qRT-PCR, quantitative real time polymerase chain reaction; TF, transcription factor; miRNA, microRNA; mRNA, messenger RNA.

Next, the overlapped differentially expressed mRNAs in the GSE110147 and GSE53845 datasets were selected as DEGs.

GSEA analysis of DEGs

To forecast the possible biological functions and pathways of these DEGs, GSEA was conducted using the clusterprofiler R package. P<0.05 was considered statistically significant.

WGCNA analysis and functional enrichment analysis

To screen an important module in DEGs, the GSE53845 microarray dataset was downloaded, and WGCNA analysis of DEGs was performed using the "WGCNA" R package. Pearson correlation was chosen to construct the network. We selected a soft-thresholding power of 8 when 0.8 was used as the correlation coefficient threshold. Also, the minimum number of module genes was 10, and the cutting height is 0.91. Next, the important module genes were used for GO analysis and KEGG pathway analysis. Here, an adjusted P value <0.05 was considered statistically significant.

TFs-miRNA-mRNA network construction

It is known that miRNA can bind to targeted mRNA to promote the degradation of mRNA. Herein, the targeted mRNAs of these miRNA signatures were obtained using the miRDB (http://www.mirdb.org), miRTarBase (https://mirtarbase.cuhk.edu.cn), and TargetScan (http://www.targetscan.org) databases. MRNAs presented in all three databases were regarded as targeted mRNAs of these miRNAs. By comparing the predicted targeted mRNAs with the DEGs, only the remaining overlapped mRNAs and their interaction miRNA-mRNA pairs were used to construct the miRNA-mRNA network.

Also, TFs can regulate the transcriptional expression of various RNAs. Therefore, TFs prediction of miRNAs in the miRNA-mRNA network was performed based on the TransmiR v2.0 database. Finally, an IPF-related TFs-miRNA-mRNA network was constructed. The predicted TFs were used for experimental verification.

GO and KEGG enrichment analysis of the TFs-miRNA-mRNA network

To forecast the possible functions and pathways of this TFs-

miRNA-mRNA network, GO and KEGG analyses were conducted using the clusterprofiler R package. P<0.05 was considered statistically significant.

Cell culture and treatment

Human embryonic lung fibroblasts (MRC-5) was purchased from Procell Life Science & Technology Co., Ltd. (Wuhan, China). For maintenance, the cells (MRC-5) were maintained in the appropriate medium [Dulbeccos Modified Eagle Medium (DMEM)] containing 10% fetal bovine serum (FBS), 100 U/mL penicillin, and 100 μg/mL streptomycin (Gibco) at 37 ℃ with 5% carbon dioxide (CO_2). Before determining the concentration, we searched lots of literature and found many studies (29-31) finally determined 5 ng/mL TGF-β1 as the optimal concentration by setting different concentration and comparing the effect of promoting fibrosis. In the pre-experiment we also set different concentration of TGF-β1 (2, 5, 10 ng/mL), and found when the concentration of TGF-β1 is 5 ng/mL, the effect of promoting fibrosis is the most significant. Therefore, fibroblasts (MRC-5) were cultured in a medium supplemented with 5 ng/mL recombinant TGF-β1 (Peprotech, New Jersey, USA) for 0, 24, and 48 h to induce fibroblast activation.

Verification of the candidate biomarkers

Firstly, total RNA was isolated from fibroblasts (MRC-5) using Trizol reagent (AG) and reverse-transcribed into complementary DNA (cDNA) using the Evo M-MLV RT Premix for qPCR kit (Accurate Biotechnology, Hunan, China). Then, the quantitative real time polymerase chain reaction (qRT-PCR) was carried out using the SYBR® Green Premix Pro Taq HS qPCR Kit (Rox Plus, Hunan, China) on the Agilent Mx 3000P machine (Agilent Technologies, California, USA) according to the manufacturer's instructions. Glyceraldehyde-3-phosphate dehydrogenase (GAPDH) was used as an endogenous control for the detection. All primers in this study are shown in Table S1. The expression levels of target TFs (relative to GAPDH) were analyzed using the $2^{-\Delta\Delta Ct}$ method.

Statistical analysis

All experiments were repeated at least in three times. Multiple group comparisons were assessed using a two-way analysis of variance (ANOVA) with Tukey's multiple comparisons test. All statistical analysis was done using GraphPad Prism 9 and P<0.05 was considered significant.

Results

DEMs and DEGs screening

The data in this study were analyzed separately (*Figure 2*). For DEMs, there were 53 differentially expressed miRNAs (30 up-regulated and 23 down-regulated) in the GSE13316 dataset. As for the DEGs, there were 15,338 differentially expressed mRNAs (6,017 up-regulated and 9,321 down-regulated) in the GSE110147 dataset, while there were 5,490 differentially expressed mRNAs (2,650 up-regulated and 2,840 down-regulated) in the GSE53845 dataset. Herein, 2,630 DEGs (1,089 up-regulated and 1,541 down-regulated) were screened. The DEMs and DEGs were used in the subsequent analyses (*Figure 3A*).

GSEA analysis of DEGs

As shown in *Figure 3B*, the GSEA analysis results indicated that these DEGs were mainly enriched in protein digestion and absorption, (extracellular matrix) ECM-receptor interaction, rheumatoid arthritis, and focal adhesion. Herein, the up-regulated genes in IPF were mainly associated with protein digestion and absorption, the phosphatidylinositol 3 kinase-protein kinase B (*PI3K-Akt*) signaling pathway, and focal adhesion, while the down-regulated genes in IPF were mainly associated with neuroactive ligand-receptor interaction and arachidonic acid metabolism.

WGCNA and functional enrichment analysis

We selected a soft-thresholding power of 8 when 0.8 was used as the correlation coefficient threshold (*Figure 4A*). Through WGCNA (2,630 genes), eight co-expression modules were constructed (*Figure 4B*), which were independent of other modules. The blue module demonstrated the highest number of genes and significant cross-clustering in the network heatmap plot.

The blue module genes (86 genes) were used for the subsequent analysis (Tables S2,S3). GO functional annotation included three sub-ontologies, namely biological process (BP), cellular component (CC), and molecular function (MF). As shown in *Figure 5A*, DEGs in the BP category were mainly associated with cilium assembly,

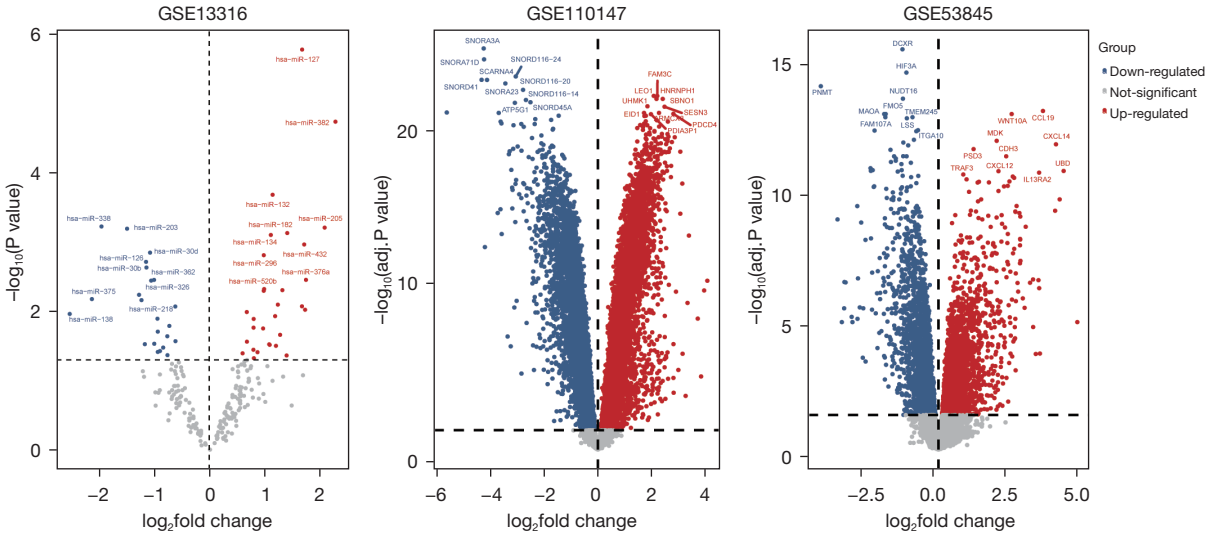

Figure 2 Volcano plot of DEMs and DEGs. Adjusted P<0.05 was used to screen for differentially expressed mRNAs, and P<0.05 was used to screen for differentially expressed microRNAs. The 10 molecules with the most significant up- and down-regulated differences are listed. DEM, differentially expressed miRNA; DEG, differentially expressed gene; mRNA, messenger RNA.

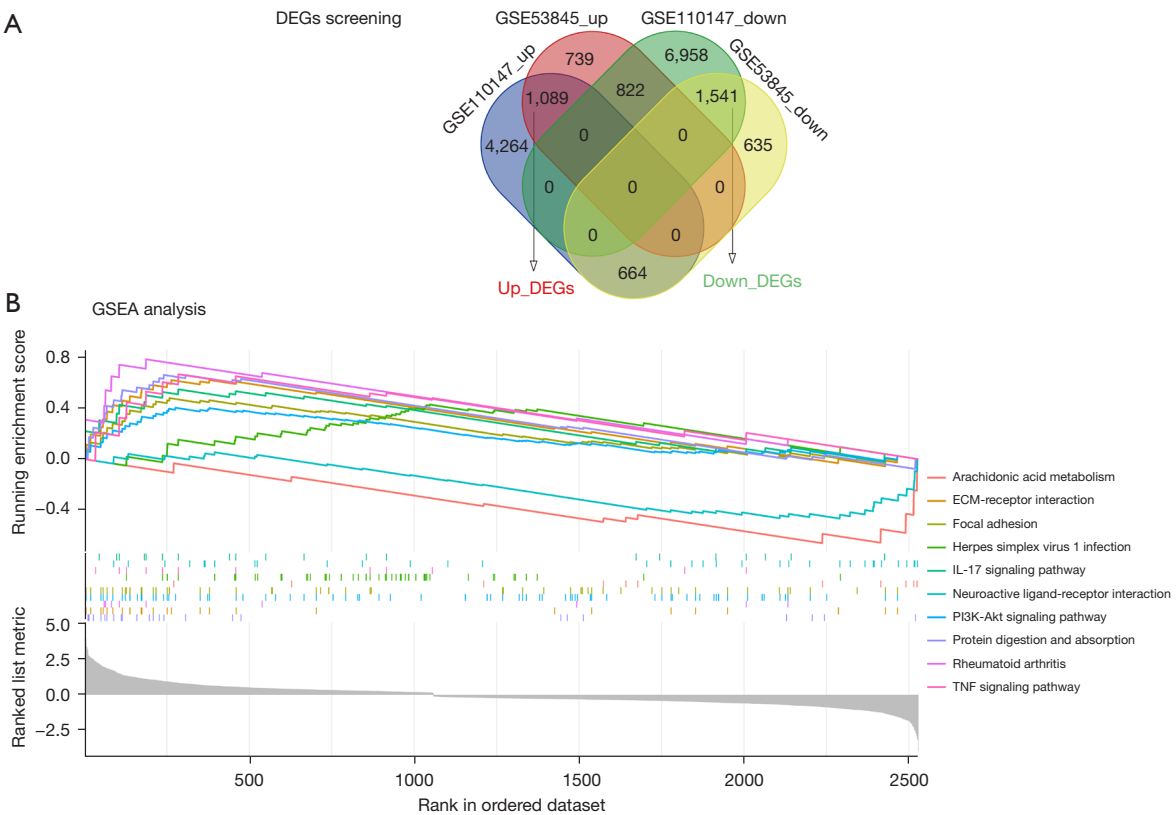

Figure 3 Screening and GSEA analysis of DEGs. (A) Screening of DEGs using the up/down-regulated differentially expressed mRNA intersection of the pulmonary fibrosis-related GEO datasets, GSE53845 and GSE110147. (B) List of the top 10 gene sets for GSEA analysis of DEGs. DEG, differentially expressed miRNA; GSEA, gene set enrichment analysis; ECM, extracellular matrix; IL, interleukin; TNF, tumor necrosis factor.

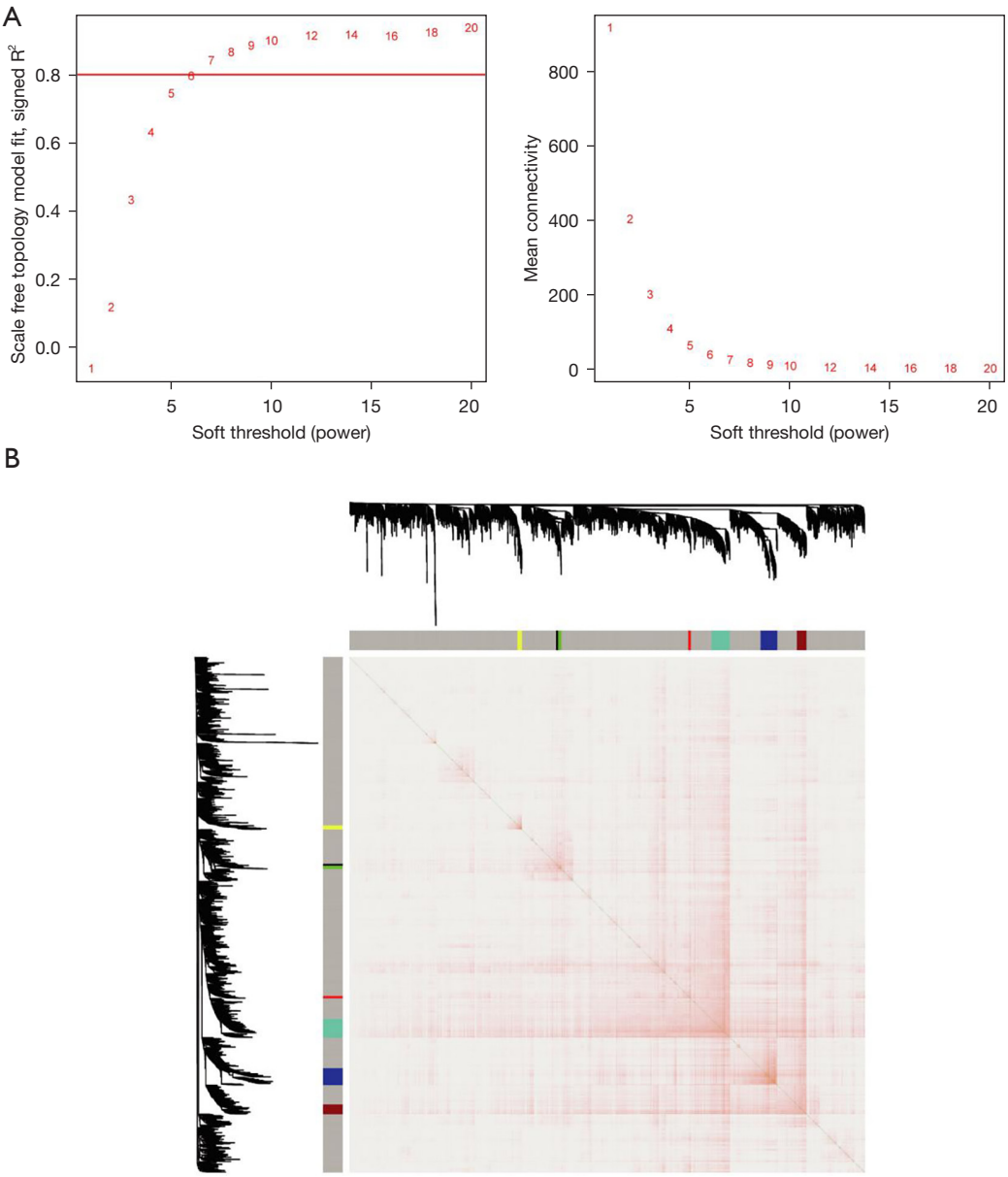

Figure 4 WGCNA analysis. (A) Analysis of the scale-free fit index for various soft-thresholding powers (left) and analysis of the mean connectivity for various soft-thresholding powers (right); (B) Network heatmap plot in the co-expression modules (the progressively saturated red colors indicated higher overlap among the functional modules). WGCNA, weighted gene co-expression network analysis.

cilium organization, and homophilic cell adhesion via plasma membrane adhesion molecules. As for the CC terms, the DEGs were mainly involved in the ciliary basal body, plasma membrane-bounded cell projection cytoplasm, and cytoplasmic region. Regarding MF, the DEGs were mainly enriched in alpha-tubulin binding, glutathione transferase activity, and integrin binding. As shown in *Figure 5B*, the KEGG pathways of the DEGs were significantly enriched in fluid shear stress and atherosclerosis, drug metabolism-cytochrome P450, xenobiotic metabolism by cytochrome P450, transcriptional dysregulation in cancer, and the interleukin (IL)-17 signaling pathway.

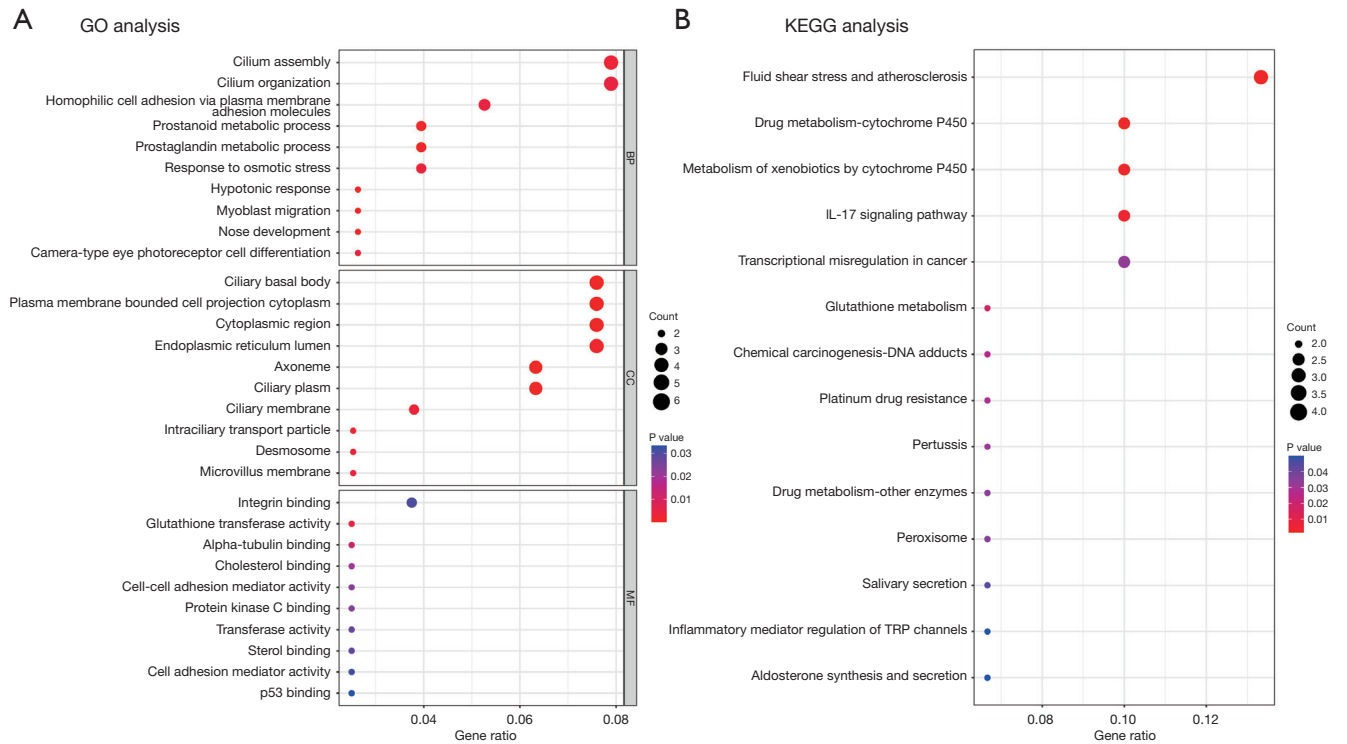

Figure 5 Functional enrichment analysis of the blue module genes. (A) GO analysis of the blue module genes. The colors represent the P value of each GO terms; red represents low while blue denotes high. (B) KEGG analysis of the blue module genes. The colors represent the P value of each GO terms; red signifies low while blue denotes high. GO, Gene Ontology; KEGG, Kyoto Encyclopedia of Genes and Genomes; IL, interleukin; BP, biological process; MF, molecular function; CC, cellular component.

TFs-miRNA-mRNA network

Using the miRDB, TargetScan, and miRTarBase databases, we took advantage of 53 DEMs for the second prediction and obtained 347 mRNAs. By overlapping these 347 predicted mRNAs and the previously screened 2,630 DEGs (1,089 up-regulated and 1,541 down-regulated), we obtained 11 miRNAs (*hsa-miR-520b*, *hsa-miR-30a-5p*, *hsa-miR-557*, *hsa-miR-198*, etc.) and 60 mRNAs (*GALNT1*, *NDEL1*, *SETD3*, *GLO1*, etc.).

As illustrated in *Figure 6A*, a TFs-miRNA-mRNA network, including 25 TFs (such as *AR*, *ARNTL*, and *CEBPA*), 11 miRNAs (*hsa-miR-520b*, *hsa-miR-30a-5p*, *hsa-miR-557*, *hsa-miR-198*, etc.), and 60 mRNAs (*GALNT1*, *NDEL1*, *SETD3*, *GLO1*, etc.), was constructed. This network suggested that these miRNAs or TFs might regulate the expression of some mRNAs in IPF, thereby playing critical roles in the genesis and development of IPF.

Functional enrichment analysis of the TFs-miRNA-mRNA network

To better understand this TFs-miRNA-mRNA network, GO functional annotation and KEGG pathway enrichment analyses were performed. GO functional annotation included three categories, namely BP, CC, and MF. The top 30 enriched GO items are listed in *Figure 6B*. The BP terms were significantly enriched in respiratory system development, microtubule nucleation, and microtubule polymerization. The CC terms were enriched in the coated vesicle, cell leading edge, and coat protein II (COPII)-coated endoplasmic reticulum (ER) to Golgi transport vesicle. The MF terms included tubulin binding and transmembrane transporter binding.

The six most important KEGG pathways are shown in *Figure 6C*, which included the cell cycle, the PI3K-Akt signaling pathway, hepatitis C, protein processing in the

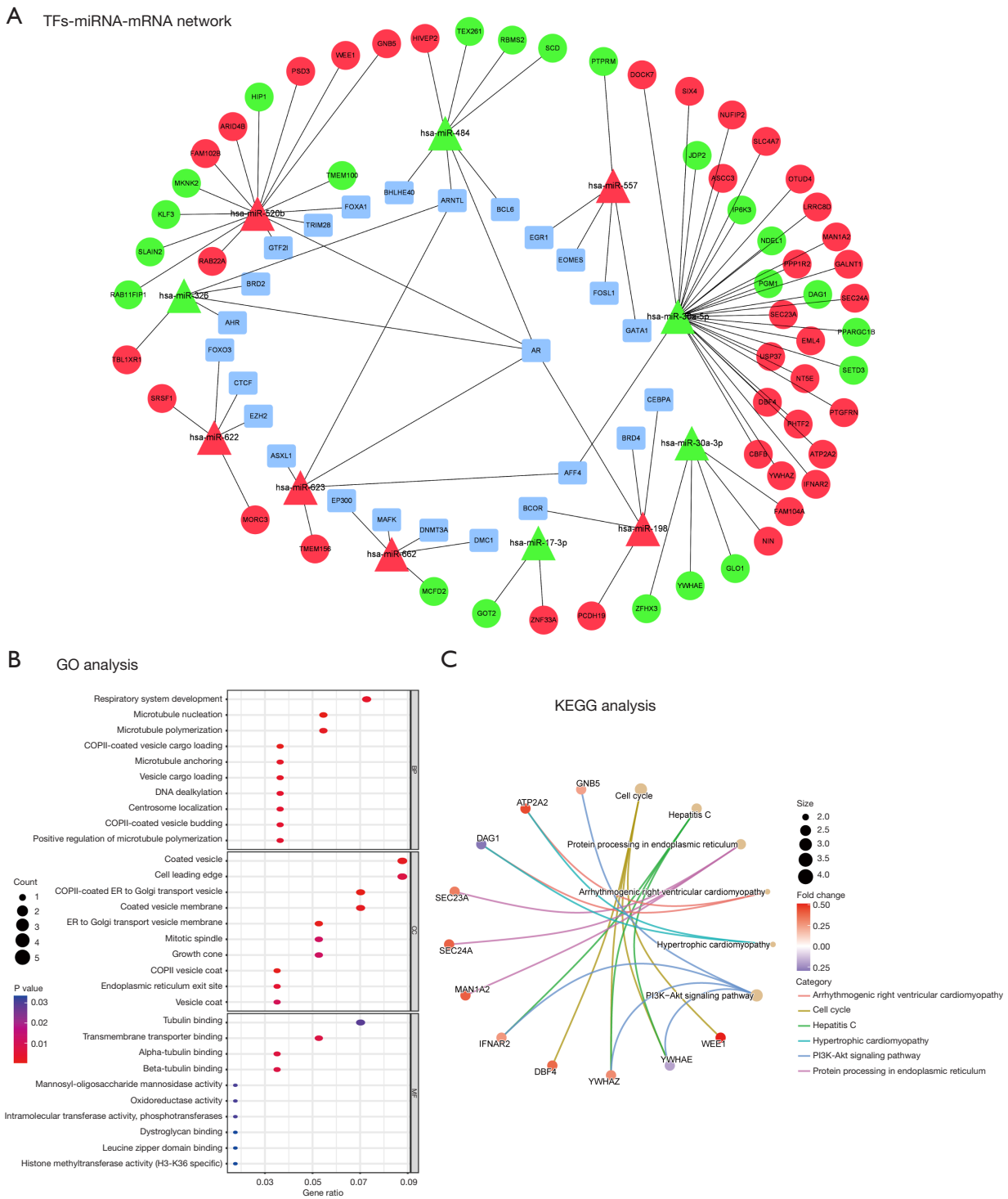

Figure 6 The TFs-miRNA-mRNA network and functional enrichment analysis. (A) The TFs-miRNA-mRNA network. (B) GO analysis of the TFs-miRNA-mRNA network. The colors represent the P value of each GO terms; red denotes low while blue signifies high. (C) KEGG analysis of the TFs-miRNA-mRNA network. TF, transcription factor; miRNA, microRNA; mRNA, messenger RNA; GO, Gene Ontology; KEGG, Kyoto Encyclopedia of Genes and Genomes; ER, endoplasmic reticulum; BP, biological process; MF, molecular function; CC, cellular component.

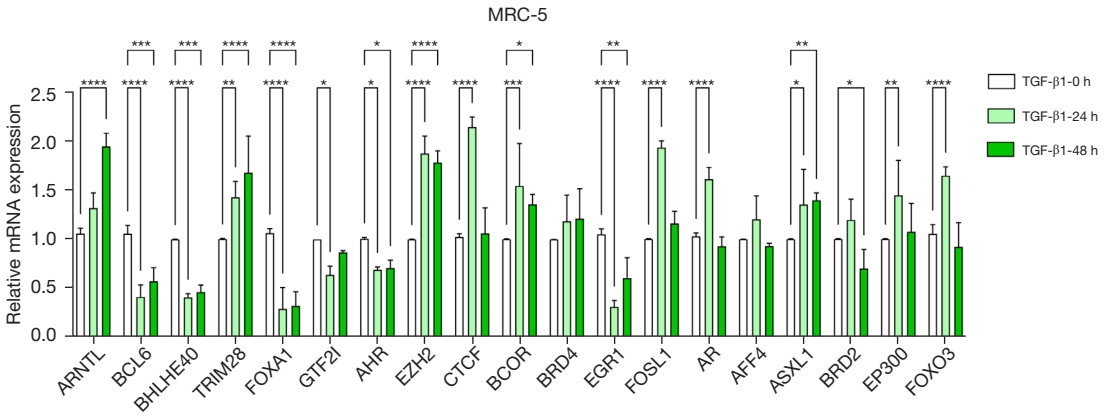

Figure 7 The qRT-PCR verification of 19 transcription factors in the TFs-miRNA-mRNA network. MRC-5 cells were treated with 5 ng/mL TGF-β1 for 0, 24, and 48 h (n=3), with ****, P<0.0001, ***, P<0.001, **, P<0.01, *, P<0.05 *vs.* the control group. MRC, human embryonic lung fibroblasts; TGF, transforming growth factor; qRT-PCR, quantitative real time polymerase chain reaction; TF, transcription factor; miRNA, microRNA; mRNA, messenger RNA.

endoplasmic reticulum, arrhythmogenic right ventricular cardiomyopathy, and hypertrophic cardiomyopathy.

Experimental verification

TGF-β1 is the most important pro-fibrotic factor and plays a key role in the pathogenesis of IPF (2,10). TGF-β1-treated fibroblasts have been used by various teams to perform *in vitro* phenotype-related studies of lung fibrosis (31-33). Hence, in the current study, validation experiments using TGF-β1 treatment were chosen. We used qRT-PCR to verify the TFs in the TFs-miRNA-mRNA network, and the experimental results are shown in *Figure* 7. Following TGF-β1 treatment, *ARNTL*, *TRIM28*, *EZH2*, *BCOR*, and *ASXL1* were statistically sufficiently up-regulated in a time-dependent manner. In addition, *BCL6*, *BHLHE40*, *FOXA1*, and *EGR1* were statistically significantly down-regulated. Meanwhile, *CTCF*, *FOSL1*, *AR*, and *FOXO3* were markedly up-regulated under TGF-β1 treatment in the 24 h groups but not in the 48 h groups.

Discussion

IPF is a chronic, progressive, fibrotic interstitial lung disease of unknown etiology that is common in elderly individuals and typically presents with characteristic imaging and histological findings (2). The psychological, physical, and socio-economic burden of IPF is substantial. With the evolution of diagnostic methods and the aging population worldwide, the prevalence and incidence rates of IPF may increase over time (34,35). The median survival of IPF patients is 2–3 years if left treated (34), and the current treatment methods are not yet satisfactory. Therefore, efforts have been made to investigate the mechanisms of IPF to discover promising therapies.

IPF is the most common type of idiopathic interstitial pneumonia, and its pathogenesis involves the dysregulation of gene networks, including both non-coding RNAs and protein-coding genes (32,36,37). Non-coding RNA lacks protein-coding ability but can still regulate a variety of cell BPs, including those related to tumorigenesis and development, aging, and the pathogenesis of IPF. In previous studies (38-40), *miR-34a* was found to be elevated in IPF tissues and inhibit cellular senescence through *SIRT1* in Alveolar epithelial cells (AECs) and fibroblasts. Another study found that the low expression of *miR-29* in IPF increases AECs antioxidants (SOD2, MnSOD, catalase) and inhibits apoptosis in AECs by regulating *FOXO3A* (41). Wang *et al.* demonstrated that long non-coding RNA *SIRT-AS1* (lncRNA *SIRT-AS1*) can inhibit the *miR-34a*-mediated targeting of *SIRT1* and hence suppress the progression of IPF (42). However, the comprehensive TFs-miRNA-mRNA network in IPF remains largely unknown, and the construction of this network will provide novel insights into the underlying molecular mechanisms of IPF.

In the present study, we analyzed the IPF-associated datasets from the GEO database. DEGs were identified between the IPF and normal lung tissues from the GSE110147 and GSE53845 datasets, and DEMs were identified between the IPF and normal lung tissues from

the GSE13316 dataset. A Venn plot was used to obtain the intersection of DEGs. Through our analysis, 53 DEMs (30 up and 23 down) and 2,630 DEGs (1,089 up and 1,541 down) were screened. GSEA was performed to explore the possible enriched gene sets of these DEGs. These genes were related to arachidonic acid metabolism, herpes simplex virus 1 infection, the TNF signaling pathway, the IL-17 signaling pathway, neuroactive ligand-receptor interaction, the *PI3K-Akt* signaling pathway, protein digestion and absorption, ECM-receptor interaction, rheumatoid arthritis, and focal adhesion. It was reported previously that the anti-hepatic fibrosis effect of curcumol was related to its regulation of arachidonic acid metabolism (43). However, whether arachidonic acid metabolism is involved in the progression of IPF requires further study. As a famous immune checkpoint marker, programmed death-1 (*PD-1*) is upregulated in Cluster of Differentiation 4 ($CD4^+$) T cells of IPF tissues, and increases the expression of the TF, signal transducer and activator of transcription 3 (*STAT3*), thereby accelerating the progression of pulmonary fibrosis by promoting the production of IL-17A and TGF-β. Our results are consistent with the previous findings, which both highlight the important role of IL-17 signaling in IPF (44).

Further, WGCNA showed that these DEGs were divided into eight modules. Turquoise module genes were utilized for GO and KEGG pathway analyses. The BP module of GO analysis showed that the blue module genes were mainly enriched in cilium-associated processes and cell adhesion, including cilium assembly, cilium organization, axoneme assembly, homophilic cell adhesion via plasma membrane adhesion molecules, cell-cell adhesion mediator activity, and myoblast migration. Interestingly, the KEGG pathway analysis showed that these genes were mainly enriched in the metabolic pathway. Glutathione metabolism, drug metabolism, and the IL-17 signaling pathway were among the top 10 pathways. Cilium-associated genes were reported to define the molecular subtypes of IPF and take part in regulating the progression of IPF (45,46). Also, glutathione S-transferases (GSTs) are reportedly enriched in pulmonary fibrosis cells and mice models. TLK117, a GSTs inhibitor, can dampen the severity of pulmonary fibrosis (47).

We used the miRDB, miRTarBase, and TargetScan databases to predict the downstream targeted mRNAs, which were then compared with DEGs to identify the overlapping mRNAs. The remaining mRNAs were applied to construct the miRNA-mRNA network. To explore the upstream TFs regulating the transcriptional expression of miRNAs, we used the TransmiR v2.0 database to build the TFs-miRNA-mRNA network. Hub miRNAs in the network included six up-regulated DEMs (*hsa-miR-520b*, *hsa-miR-557*, *hsa-miR-198*, *hsa-miR-662*, *hsa-miR-623*, and *hsa-miR-622*) and five downregulated DEMs (*hsa-miR-484*, *hsa-miR-30a-5p*, *hsa-miR-30a-3p*, *hsa-miR-17-3p*, and *hsa-miR-326*). Among these hub miRNAs, *has-miR-30a-5p* had the maximum branches and nodes, indicating that it may play an important role in the regulation of pulmonary fibrosis. Mao *et al.* found that *miR-30a* inhibits tet methylcytosine dioxygenase 1 (*TET1*) expression via base pairing with complementary sites in the 3'-untranslated region (3'UTR) to modulate dynamin-related protein-1 (*Drp-1*)-promoter hydroxymethylation. Hence, *miR-30a* acts as a potential therapeutic target of IPF by blocking mitochondrial fission, which is dependent on *Drp-1* (48).

MicroRNA 17-92 (*MiR17-92*) is down-regulated in lung fibroblasts of IPF tissues compared with control tissues; the DNA methylation degree of its promotor and DNA methyltransferase 1 (*DNMT1*) expression increase synchronously. There is also a feedback loop between *DNMT1* and *microRNA 17-92* (*miR17-92*) in lung fibrosis (49). Das *et al.* demonstrated that *miR-326* can down-regulate profibrotic genes such as *SMAD* family member 3 (*Smad3*), matrix metallopeptidase 9 (*MMP9*), and ETS proto-oncogene 1 (*Ets1*) and increase the expression of antifibrotic genes such as *Smad*7 (50). The significant decrease in *miR-484* in the lung tissue or plasma of bleomycin-administered mice suggests that it could be a possible indicator of drug-induced pulmonary fibrosis (51). Our results are consistent with these previous findings, and we also found that there are limited studies on *miR-520b*, *miR-557*, *miR-198*, *miR-662*, *miR-623*, and *miR-622* in the pathogenesis of IPF.

The network indicates that common upstream TFs, such as the androgen receptor (*AR*), may regulate hub miRNAs. Androgen and ARs are regulators of macrophages and monocytes in diseased lungs, such as those in asthma, chronic obstructive pulmonary disease, and lung cancer (52). To our knowledge, IPF is a lung disease that manifests sex differences (53), with higher incidence and severity in males (54-56). Additionally, the expression of ARs is greater in macrophages in males than in females (57). In the current study, *AR* was statistically significantly up-regulated under TGF-β1 treatment in the 24 h groups, but not in the 48 h groups. However, advanced research is required to determine whether AR is an important regulator in IPF pathogenesis. Another common TF is aryl hydrocarbon

receptor nuclear translocator like (*ARNTL*), which is a transcriptional activator of the molecular clock feedback network that is involved in the modulation of generating circadian rhythms, cell proliferation, autophagy, and cancer cell invasion. Dong *et al.* showed that downregulating the expression of *ARNTL* significantly inhibited the canonical *TGF-β1* signaling pathway and modulated TGF-β1-induced epithelial-mesenchymal transition in lung epithelial cells (58). Enhancer of zeste homolog 2 (*EZH2*) is the key catalytic subunit of polycomb repressive complex 2 (*PRC2*), which can regulate downstream gene expression via trimethylation of H3K27me3 (trimethylation at lysine 27 of histone H3). The interplay between the epigenetic regulators *EZH2* and G9a is reportedly responsible for suppressing the expression of the antifibrotic factors, cytochrome c oxidase subunit II (*COX2*) and C-X-C motif chemokine ligand 10 (*CXCL10*), in IPF via H3K27me3 and H3K9me3 (59,60). Another study reported that treatment with *EZH2* inhibitors could suppress M1 macrophages while promoting M2 macrophage differentiation by activating peroxisome proliferator-activated receptor (*PPAR*)-γ and modulating the signal transducer and activator of transcription/ suppressor of cytokine signaling (*STAT/SOCS*) pathway (61). MicroRNA-224 (*miR-224*) and its target forkhead box A1 (*FOXA1*) inhibit the expression of EMT markers and the migration and invasion of human lung fibroblasts in IPF under hypoxia (62). Bromodomain containing 4 (*BRD4*) plays a critical role in promoting pulmonary myofibroblast activation and redox imbalance, and *BRD4* inhibitors is capable of inhibiting the profibrotic effects of IPF and attenuates bleomycin-induced lung fibrosis in mice (63,64). E1A binding protein p300 (*EP300*) is another important transcription factor in the network. In bronchial epithelial cells of IPF, *EP300* were up-regulated and involved in the regulation of autophagy, cellular response to organonitrogen compounds, and collagen metabolic pathways (65). The role of forkhead box O3 (*FOXO3*) in pulmonary fibrosis is controversial. Qian *et al.* reported that overexpression of *FOXO3* could reverse the antifibrosis effects induced by Angelica sinensis polysaccharide treatment (66). Lee *et al.* found that chitinase 1 (*CHIT1*) could regulate pulmonary fibrosis by modulating the *TGF-β1/SMAD7* axis via interaction with *FOXO3* and *TGF-β* receptor-associated protein 1 (*TGFBRAP1*) (67). However, another researcher found that *FOXO3* was less expressed relative to the non-diseased controls. The knockout of *FOXO3* displayed increased susceptibility to bleomycin challenge, with augmented fibrosis and higher mortality in mice (68).

MRNAs in the network were selected for GO analysis. Among the top 10 BPs, mitosis-related pathways accounted for half. A genetic study involving 1,725 IPF patients and 23,509 controls found heterozygous deleterious variants in kinesin family member 15 (*KIF15*), which take part in spindle separation during mitosis (69). Mitotic imbalance may be an important mechanism in the pathogenesis of IPF. The six most important pathways analyzed by KEGG included the cell cycle, the *PI3K-Akt* signaling pathway, hepatitis C, protein processing in the endoplasmic reticulum, arrhythmogenic right ventricular cardiomyopathy, and hypertrophic cardiomyopathy. Numerous reports have indicated that the *PI3K-Akt* signaling pathway plays an important role in the pulmonary fibrosis process. In recent years, various research teams have utilized *PI3K/AKT* pathway inhibitors in animal models (70) and clinical trials (71) to investigate their effects on the process of pulmonary fibrosis, and they have achieved important results. The administration of a pathway inhibitor in a mouse model of IPF was shown to significantly inhibit *PI3K* activation and suppress the production of hydroxyproline, thereby reducing collagen deposition and ultimately improving mouse survival.

Our research still has certain limitations that should be noted. Firstly, the data used in this study came from the GEO public database; for retrospective analysis, this level of evidence is insufficient. Secondly, the regulatory network lacks expression verification in *in vivo* models, and thus, in-depth mechanism research should be conducted after verifying the definite expression correlation.

Conclusions

The novel TFs-miRNA-mRNA network that we constructed could provide new insights into the underlying molecular mechanisms of IPF. *ARNTL*, *TRIM28*, *EZH2*, *BCOR*, *ASXL1*, *BCL6*, *BHLHE40*, *FOXA1*, and *EGR1* may play important roles in IPF and become effective biomarkers for diagnosis and treatment.

Acknowledgments

The results shown in the current study are mainly based on data obtained from the Gene Expression Omnibus (https://www.ncbi.nlm.nih.gov/gds/).

Funding: This work was supported by grants from the National Natural Science Foundation of China (Grant

No. 81902559), the Guangdong Basic and Applied Basic Research Foundation (Grant No. 2019A1515110787), and the Dean's Foundation of Zhujiang Hospital of Southern Medical University (Grant Nos. yzjj2018rc08 and yzjj2021qn14).

Footnote

Reporting Checklist: The authors have completed the STREGA reporting checklist. Available at https://atm.amegroups.com/article/view/10.21037/atm-22-6161/rc

Data Sharing Statement: Available at https://atm.amegroups.com/article/view/10.21037/atm-22-6161/dss

Conflicts of Interest: All authors have completed the ICMJE uniform disclosure form (available at https://atm.amegroups.com/article/view/10.21037/atm-22-6161/coif). The authors have no conflicts of interest to declare.

Ethical Statement: The authors are accountable for all aspects of the work in ensuring that questions related to the accuracy or integrity of any part of the work are appropriately investigated and resolved. The study was conducted in accordance with the Declaration of Helsinki (as revised in 2013).

References

1. Raghu G, Collard HR, Egan JJ, et al. An official ATS/ERS/JRS/ALAT statement: idiopathic pulmonary fibrosis: evidence-based guidelines for diagnosis and management. Am J Respir Crit Care Med 2011;183:788-824.
2. Lederer DJ, Martinez FJ. Idiopathic Pulmonary Fibrosis. N Engl J Med 2018;378:1811-23.
3. Vancheri C, Failla M, Crimi N, et al. Idiopathic pulmonary fibrosis: a disease with similarities and links to cancer biology. Eur Respir J 2010;35:496-504.
4. Natsuizaka M, Chiba H, Kuronuma K, et al. Epidemiologic survey of Japanese patients with idiopathic pulmonary fibrosis and investigation of ethnic differences. Am J Respir Crit Care Med 2014;190:773-9.
5. Navaratnam V, Fleming KM, West J, et al. The rising incidence of idiopathic pulmonary fibrosis in the U.K. Thorax 2011;66:462-7.
6. Nalysnyk L, Cid-Ruzafa J, Rotella P, et al. Incidence and prevalence of idiopathic pulmonary fibrosis: review of the literature. Eur Respir Rev 2012;21:355-61.
7. Hutchinson J, Fogarty A, Hubbard R, et al. Global incidence and mortality of idiopathic pulmonary fibrosis: a systematic review. Eur Respir J 2015;46:795-806.
8. Selman M, King TE, Pardo A, et al. Idiopathic pulmonary fibrosis: prevailing and evolving hypotheses about its pathogenesis and implications for therapy. Ann Intern Med 2001;134:136-51.
9. Raghu G, Anstrom KJ, et al. Prednisone, azathioprine, and N-acetylcysteine for pulmonary fibrosis. N Engl J Med 2012;366:1968-77.
10. Richeldi L, Collard HR, Jones MG. Idiopathic pulmonary fibrosis. Lancet 2017;389:1941-52.
11. Tian L, Cao J, Deng X, et al. Unveiling transcription factor regulation and differential co-expression genes in Duchenne muscular dystrophy. Diagn Pathol 2014;9:210.
12. Bhattacharyya S, Wu M, Fang F, et al. Early growth response transcription factors: key mediators of fibrosis and novel targets for anti-fibrotic therapy. Matrix Biol 2011;30:235-42.
13. Cadena-Suárez AR, Hernández-Hernández HA, Alvarado-Vásquez N, et al. Role of MicroRNAs in Signaling Pathways Associated with the Pathogenesis of Idiopathic Pulmonary Fibrosis: A Focus on Epithelial-Mesenchymal Transition. Int J Mol Sci 2022;23:6613.
14. Ye Z, Hu Y. TGF-β1: Gentlemanly orchestrator in idiopathic pulmonary fibrosis (Review). Int J Mol Med 2021;48:132.
15. Huang Y, Xie Y, Abel PW, et al. TGF-β1-induced miR-424 promotes pulmonary myofibroblast differentiation by targeting Slit2 protein expression. Biochem Pharmacol 2020;180:114172.
16. Deng X, Jin K, Li Y, et al. Platelet-Derived Growth Factor and Transforming Growth Factor β1 Regulate ARDS-Associated Lung Fibrosis Through Distinct Signaling Pathways. Cell Physiol Biochem 2015;36:937-46.
17. Kadoya K, Togo S, Tulafu M, et al. Specific Features of

Fibrotic Lung Fibroblasts Highly Sensitive to Fibrotic Processes Mediated via TGF-β-ERK5 Interaction. Cell Physiol Biochem 2019;52:822-37.
18. Ghatak S, Markwald RR, Hascall VC, et al. Transforming growth factor β1 (TGFβ1) regulates CD44V6 expression and activity through extracellular signal-regulated kinase (ERK)-induced EGR1 in pulmonary fibrogenic fibroblasts. J Biol Chem 2017;292:10465-89.
19. Pandit KV, Corcoran D, Yousef H, et al. Inhibition and role of let-7d in idiopathic pulmonary fibrosis. Am J Respir Crit Care Med 2010;182:220-9.
20. Strell C, Norberg KJ, Mezheyeuski A, et al. Stroma-regulated HMGA2 is an independent prognostic marker in PDAC and AAC. Br J Cancer 2017;117:65-77.
21. Thuault S, Valcourt U, Petersen M, et al. Transforming growth factor-beta employs HMGA2 to elicit epithelial-mesenchymal transition. J Cell Biol 2006;174:175-83.
22. Liu G, Friggeri A, Yang Y, et al. miR-21 mediates fibrogenic activation of pulmonary fibroblasts and lung fibrosis. J Exp Med 2010;207:1589-97.
23. Yang S, Banerjee S, de Freitas A, et al. Participation of miR-200 in pulmonary fibrosis. Am J Pathol 2012;180:484-93.
24. Zhu K, Xu A, Xia W, et al. Integrated analysis of the molecular mechanisms in idiopathic pulmonary fibrosis. Int J Med Sci 2021;18:3412-24.
25. Wu T, Hu E, Xu S, et al. clusterProfiler 4.0: A universal enrichment tool for interpreting omics data. Innovation (Camb) 2021;2:100141.
26. Langfelder P, Horvath S. WGCNA: an R package for weighted correlation network analysis. BMC Bioinformatics 2008;9:559.
27. Kanehisa M, Goto S. KEGG: kyoto encyclopedia of genes and genomes. Nucleic Acids Res 2000;28:27-30.
28. Kanehisa M, Furumichi M, Sato Y, et al. KEGG: integrating viruses and cellular organisms. Nucleic Acids Res 2021;49:D545-51.
29. Gu L, Zhu YJ, Yang X, et al. Effect of TGF-beta/Smad signaling pathway on lung myofibroblast differentiation. Acta Pharmacol Sin 2007;28:382-91.
30. Zhang Q, Tu W, Tian K, et al. Sirtuin 6 inhibits myofibroblast differentiation via inactivating transforming growth factor-β1/Smad2 and nuclear factor-κB signaling pathways in human fetal lung fibroblasts. J Cell Biochem 2019;120:93-104.
31. Xu Q, Cheng D, Li G, et al. CircHIPK3 regulates pulmonary fibrosis by facilitating glycolysis in miR-30a-3p/FOXK2-dependent manner. Int J Biol Sci 2021;17:2294-307.
32. Li J, Li P, Zhang G, et al. CircRNA TADA2A relieves idiopathic pulmonary fibrosis by inhibiting proliferation and activation of fibroblasts. Cell Death Dis 2020;11:553.
33. Liu P, Luo G, Dodson M, et al. The NRF2-LOC344887 signaling axis suppresses pulmonary fibrosis. Redox Biol 2021;38:101766.
34. Maher TM, Bendstrup E, Dron L, et al. Global incidence and prevalence of idiopathic pulmonary fibrosis. Respir Res 2021;22:197.
35. Diamantopoulos A, Wright E, Vlahopoulou K, et al. The Burden of Illness of Idiopathic Pulmonary Fibrosis: A Comprehensive Evidence Review. Pharmacoeconomics 2018;36:779-807.
36. Zhou J, Lin Y, Kang X, et al. microRNA-186 in extracellular vesicles from bone marrow mesenchymal stem cells alleviates idiopathic pulmonary fibrosis via interaction with SOX4 and DKK1. Stem Cell Res Ther 2021;12:96.
37. Yi H, Luo D, Xiao Y, Jiang D. Knockdown of long non-coding RNA DLEU2 suppresses idiopathic pulmonary fibrosis by regulating the microRNA-369-3p/TRIM2 axis. Int J Mol Med 2021;47:80.
38. Cui H, Ge J, Xie N, et al. miR-34a promotes fibrosis in aged lungs by inducing alveolarepithelial dysfunctions. Am J Physiol Lung Cell Mol Physiol 2017;312:L415-24.
39. Cui H, Ge J, Xie N, et al. miR-34a Inhibits Lung Fibrosis by Inducing Lung Fibroblast Senescence. Am J Respir Cell Mol Biol 2017;56:168-78.
40. Disayabutr S, Kim EK, Cha SI, et al. miR-34 miRNAs Regulate Cellular Senescence in Type II Alveolar Epithelial Cells of Patients with Idiopathic Pulmonary Fibrosis. PLoS One 2016;11:e0158367.
41. Xie T, Liang J, Geng Y, et al. MicroRNA-29c Prevents Pulmonary Fibrosis by Regulating Epithelial Cell Renewal and Apoptosis. Am J Respir Cell Mol Biol 2017;57:721-32.
42. Wang Y, Pang WJ, Wei N, et al. Identification, stability and expression of Sirt1 antisense long non-coding RNA. Gene 2014;539:117-24.
43. Zheng Y, Wang J, Wang J, et al. Gut microbiota combined with metabolomics reveal the mechanism of curcumol on liver fibrosis in mice. Biomed Pharmacother 2022;152:113204.
44. Celada LJ, Kropski JA, Herazo-Maya JD, et al. PD-1 up-regulation on CD4(+) T cells promotes pulmonary fibrosis through STAT3-mediated IL-17A and TGF-β1 production. Sci Transl Med 2018;10:eaar8356.

45. McDonough JE, Kaminski N, Thienpont B, et al. Gene correlation network analysis to identify regulatory factors in idiopathic pulmonary fibrosis. Thorax 2019;74:132-40.
46. Yang IV, Coldren CD, Leach SM, et al. Expression of cilium-associated genes defines novel molecular subtypes of idiopathic pulmonary fibrosis. Thorax 2013;68:1114-21.
47. He N, Bai S, Huang Y, et al. Evaluation of Glutathione S-Transferase Inhibition Effects on Idiopathic Pulmonary Fibrosis Therapy with a Near-Infrared Fluorescent Probe in Cell and Mice Models. Anal Chem 2019;91:5424-32.
48. Mao C, Zhang J, Lin S, et al. MiRNA-30a inhibits AECs-II apoptosis by blocking mitochondrial fission dependent on Drp-1. J Cell Mol Med 2014;18:2404-16.
49. Dakhlallah D, Batte K, Wang Y, et al. Epigenetic regulation of miR-17~92 contributes to the pathogenesis of pulmonary fibrosis. Am J Respir Crit Care Med 2013;187:397-405.
50. Das S, Kumar M, Negi V, et al. MicroRNA-326 regulates profibrotic functions of transforming growth factor-β in pulmonary fibrosis. Am J Respir Cell Mol Biol 2014;50:882-92.
51. Konaka T, Kawami M, Yamamoto A, et al. miR-484: A Possible Indicator of Drug-Induced Pulmonary Fibrosis. J Pharm Pharm Sci 2020;23:486-95.
52. Becerra-Diaz M, Song M, Heller N. Androgen and Androgen Receptors as Regulators of Monocyte and Macrophage Biology in the Healthy and Diseased Lung. Front Immunol 2020;11:1698.
53. Han MK, Murray S, Fell CD, et al. Sex differences in physiological progression of idiopathic pulmonary fibrosis. Eur Respir J 2008;31:1183-8.
54. Mortimer KM, Bartels DB, Hartmann N, et al. Characterizing Health Outcomes in Idiopathic Pulmonary Fibrosis using US Health Claims Data. Respiration 2020;99:108-18.
55. Olson AL, Swigris JJ, Lezotte DC, et al. Mortality from pulmonary fibrosis increased in the United States from 1992 to 2003. Am J Respir Crit Care Med 2007;176:277-84.
56. Gribbin J, Hubbard RB, Le Jeune I, et al. Incidence and mortality of idiopathic pulmonary fibrosis and sarcoidosis in the UK. Thorax 2006;61:980-5.
57. McCrohon JA, Death AK, Nakhla S, et al. Androgen receptor expression is greater in macrophages from male than from female donors. A sex difference with implications for atherogenesis. Circulation 2000;101:224-6.
58. Dong C, Gongora R, Sosulski ML, et al. Regulation of transforming growth factor-beta1 (TGF-β1)-induced pro-fibrotic activities by circadian clock gene BMAL1. Respir Res 2016;17:4.
59. Coward WR, Brand OJ, Pasini A, et al. Interplay between EZH2 and G9a Regulates CXCL10 Gene Repression in Idiopathic Pulmonary Fibrosis. Am J Respir Cell Mol Biol 2018;58:449-60.
60. Coward WR, Feghali-Bostwick CA, Jenkins G, et al. A central role for G9a and EZH2 in the epigenetic silencing of cyclooxygenase-2 in idiopathic pulmonary fibrosis. FASEB J 2014;28:3183-96.
61. Bao X, Liu X, Liu N, et al. Inhibition of EZH2 prevents acute respiratory distress syndrome (ARDS)-associated pulmonary fibrosis by regulating the macrophage polarization phenotype. Respir Res 2021;22:194.
62. Jeong SH, Son ES, Lee YE, et al. Histone deacetylase 3 promotes alveolar epithelial-mesenchymal transition and fibroblast migration under hypoxic conditions. Exp Mol Med 2022;54:922-31.
63. Tang X, Peng R, Phillips JE, et al. Assessment of Brd4 inhibition in idiopathic pulmonary fibrosis lung fibroblasts and in vivo models of lung fibrosis. Am J Pathol 2013;183:470-9.
64. Stock CJW, Michaeloudes C, Leoni P, et al. Bromodomain and Extraterminal (BET) Protein Inhibition Restores Redox Balance and Inhibits Myofibroblast Activation. Biomed Res Int 2019;2019:1484736.
65. Tao J, Zhang M, Wen Z, et al. Inhibition of EP300 and DDR1 synergistically alleviates pulmonary fibrosis in vitro and in vivo. Biomed Pharmacother 2018;106:1727-33.
66. Qian W, Cai X, Qian Q, et al. Angelica Sinensis Polysaccharide Suppresses Epithelial-Mesenchymal Transition and Pulmonary Fibrosis via a DANCR/AUF-1/FOXO3 Regulatory Axis. Aging Dis 2020;11:17-30.
67. Lee CM, He CH, Park JW, et al. Chitinase 1 regulates pulmonary fibrosis by modulating TGF-β/SMAD7 pathway via TGFBRAP1 and FOXO3. Life Sci Alliance 2019;2:e201900350.
68. Al-Tamari HM, Dabral S, Schmall A, et al. FoxO3 an important player in fibrogenesis and therapeutic target for idiopathic pulmonary fibrosis. EMBO Mol Med 2018;10:276-93.
69. Zhang D, Povysil G, Kobeissy PH, et al. Rare and Common Variants in KIF15 Contribute to Genetic Risk of Idiopathic Pulmonary Fibrosis. Am J Respir Crit Care Med 2022;206:56-69.
70. Hettiarachchi SU, Li YH, Roy J, et al. Targeted inhibition

of PI3 kinase/mTOR specifically in fibrotic lung fibroblasts suppresses pulmonary fibrosis in experimental models. Sci Transl Med 2020;12:eaay3724.
71. Lukey PT, Harrison SA, Yang S, et al. A randomised, placebo-controlled study of omipalisib (PI3K/mTOR) in idiopathic pulmonary fibrosis. Eur Respir J 2019;53:1801992.

(English Language Editor: A. Kassem)

Cite this article as: Su M, Liu J, Wu X, Chen X, Xiao Q, Jiang N. Construction of a TFs-miRNA-mRNA network related to idiopathic pulmonary fibrosis. Ann Transl Med 2023;11(2):78. doi: 10.21037/atm-22-6161

Supplementary

Table S1 qRT-PCR primer

Gene Symbol	Forward Primer	Reverse Primer
ARNTL	AAGGGAAGCTCACAGTCAGAT	GGACATTGCGTTGCATGTTGG
BCL6	ACACATCTCGGCTCAATTTGC	AGTGTCCACAACATGCTCCAT
BHLHE40	ACACATCTCGGCTCAATTTGC	AGTGTCCACAACATGCTCCAT
TRIM28	TGAGACCTGTGTAGAGGCG	CGTTCACCATCCCGAGACTT
FOXA1	GCAATACTCGCCTTACGGCT	TACACACCTTGGTAGTACGCC
GTF2I	TTGTCGTCGGAACTGAAAGAG	CGATTTGCCTGGGTTGTAGAT
AHR	ACATCACCTACGCCAGTCG	CGCTTGGAAGGATTTGACTTGA
EZH2	AATCAGAGTACATGCGACTGAGA	GCTGTATCCTTCGCTGTTTCC
CTCF	ATGTGCGATTACGCCAGTGTA	TGAAACGGACGCTCTCCAGTA
BCOR	TGGTGACGCTTCAAAAGCCA	GCTAGAATAGACGATGTTTCCCG
BRD4	ACCTCCAACCCTAACAAGCC	TTTCCATAGTGTCTTGAGCACC
EGR1	GGTCAGTGGCCTAGTGAGC	GTGCCGCTGAGTAAATGGGA
FOSL1	CAGGCGGAGACTGACAAACTG	TCCTTCCGGGATTTTGCAGAT
AR	GACGACCAGATGGCTGTCATT	GGGCGAAGTAGAGCATCCT
AFF4	AAAGGCCAGCATGGATCAGAA	GTGATTTGGAGCGTTGATGTTC
ASXL1	CGCGCCTGGTATTAGAAAACT	GCATCCTTCTTGAGCGTGAAAAG
BRD2	GAGGTGTCCAATCCCAAAAAGC	ATGCGAACTGATGTTTCCACA
EP300	AGCCAAGCGGCCTAAACTC	TCACCACCATTGGTTAGTCCC
FOXO3	CGGACAAACGGCTCACTCT	GGACCCGCATGAATCGACTAT

qRT-PCR, quantitative real time polymerase chain reaction.

https://dx.doi.org/10.21037/atm-22-6161

Table S2 GO analysis of blue module genes

ONTOLOGY	ID	Description	Gene Ratio	BgRatio	p value	p.adjust	q value	Gene ID	Count
BP	GO:0006971	hypotonic response	2/77	11/18800	0.000889	0.363992	0.351502	SLC4A1/TRPV4	2
BP	GO:0006692	prostanoid metabolic process	3/77	50/18800	0.001127	0.363992	0.351502	GSTA1/PIBF1/DAGLB	3
BP	GO:0006693	prostaglandin metabolic process	3/77	50/18800	0.001127	0.363992	0.351502	GSTA1/PIBF1/DAGLB	3
BP	GO:0051451	myoblast migration	2/77	13/18800	0.001254	0.363992	0.351502	NET1/SIX4	2
BP	GO:0043584	nose development	2/77	14/18800	0.001459	0.363992	0.351502	RPGRIP1L/SIX4	2
BP	GO:0060271	cilium assembly	6/77	355/18800	0.003342	0.437601	0.422586	WDR35/DZIP1L/PIBF1/UBXN10/BBS5/RPGRIP1L	6
BP	GO:0006970	response to osmotic stress	3/77	79/18800	0.004178	0.437601	0.422586	SLC4A11/TRPV4/SORD	3
BP	GO:0060219	camera-type eye photoreceptor cell differentiation	2/77	25/18800	0.004673	0.437601	0.422586	PROM1/RPGRIP1L	2
BP	GO:0044782	cilium organization	6/77	384/18800	0.004894	0.437601	0.422586	WDR35/DZIP1L/PIBF1/UBXN10/BBS5/RPGRIP1L	6
BP	GO:0007156	homophilic cell adhesion via plasma membrane adhesion molecules	4/77	168/18800	0.005018	0.437601	0.422586	DSG3/DSC3/CDH26/IGSF9	4
BP	GO:0045104	intermediate filament cytoskeleton organization	3/77	88/18800	0.005648	0.437601	0.422586	KRT5/KRT15/DST	3
BP	GO:0045103	intermediate filament-based process	3/77	89/18800	0.005828	0.437601	0.422586	KRT5/KRT15/DST	3
BP	GO:0035116	embryonic hindlimb morphogenesis	2/77	28/18800	0.005842	0.437601	0.422586	TP63/RPGRIP1L	2
BP	GO:0021591	ventricular system development	2/77	30/18800	0.006687	0.437601	0.422586	MNAT1/RPGRIP1L	2
BP	GO:0035115	embryonic forelimb morphogenesis	2/77	31/18800	0.00713	0.437601	0.422586	TP63/RPGRIP1L	2
BP	GO:0060351	cartilage development involved in endochondral bone morphogenesis	2/77	31/18800	0.00713	0.437601	0.422586	MMP13/TRPV4	2
BP	GO:0001516	prostaglandin biosynthetic process	2/77	32/18800	0.007585	0.437601	0.422586	PIBF1/DAGLB	2
BP	GO:0046457	prostanoid biosynthetic process	2/77	32/18800	0.007585	0.437601	0.422586	PIBF1/DAGLB	2
BP	GO:0060795	cell fate commitment involved in formation of primary germ layer	2/77	32/18800	0.007585	0.437601	0.422586	EYA2/SOX2	2
BP	GO:0035137	hindlimb morphogenesis	2/77	35/18800	0.009027	0.437601	0.422586	TP63/RPGRIP1L	2
BP	GO:0021532	neural tube patterning	2/77	36/18800	0.009533	0.437601	0.422586	DZIP1L/RPGRIP1L	2
BP	GO:0006805	xenobiotic metabolic process	3/77	108/18800	0.009913	0.437601	0.422586	GSTA1/ALDH3A1/GSTA2	3
BP	GO:0035136	forelimb morphogenesis	2/77	38/18800	0.010581	0.437601	0.422586	TP63/RPGRIP1L	2
BP	GO:0001676	long-chain fatty acid metabolic process	3/77	111/18800	0.010677	0.437601	0.422586	GSTA1/SLC27A2/DAGLB	3
BP	GO:0071470	cellular response to osmotic stress	2/77	39/18800	0.011124	0.437601	0.422586	SLC4A11/TRPV4	2
BP	GO:0033559	unsaturated fatty acid metabolic process	3/77	115/18800	0.011748	0.437601	0.422586	GSTA1/PIBF1/DAGLB	3
BP	GO:0035019	somatic stem cell population maintenance	2/77	43/18800	0.013414	0.437601	0.422586	TP63/SOX2	2
BP	GO:0045214	sarcomere organization	2/77	43/18800	0.013414	0.437601	0.422586	SIX4/FHOD3	2
BP	GO:0006690	icosanoid metabolic process	3/77	121/18800	0.013465	0.437601	0.422586	GSTA1/PIBF1/DAGLB	3
BP	GO:0001754	eye photoreceptor cell differentiation	2/77	45/18800	0.014629	0.437601	0.422586	PROM1/RPGRIP1L	2
BP	GO:0001655	urogenital system development	5/77	352/18800	0.014732	0.437601	0.422586	PROM1/TP63/HSPB11/RPGRIP1L/SIX4	5
BP	GO:0051402	neuron apoptotic process	4/77	241/18800	0.017194	0.437601	0.422586	PTPRZ1/CHL1/TP63/SIX4	4
BP	GO:0006636	unsaturated fatty acid biosynthetic process	2/77	52/18800	0.019237	0.437601	0.422586	PIBF1/DAGLB	2
BP	GO:0007224	smoothened signaling pathway	3/77	140/18800	0.019808	0.437601	0.422586	DZIP1L/HSPB11/RPGRIP1L	3
BP	GO:0043524	negative regulation of neuron apoptotic process	3/77	145/18800	0.021708	0.437601	0.422586	PTPRZ1/CHL1/SIX4	3
BP	GO:0043903	regulation of biological process involved in symbiotic interaction	2/77	56/18800	0.022109	0.437601	0.422586	TMPRSS4/CXCL6	2
BP	GO:0031122	cytoplasmic microtubule organization	2/77	57/18800	0.022853	0.437601	0.422586	DST/TRPV4	2
BP	GO:0046456	icosanoid biosynthetic process	2/77	57/18800	0.022853	0.437601	0.422586	PIBF1/DAGLB	2
BP	GO:0060042	retina morphogenesis in camera-type eye	2/77	57/18800	0.022853	0.437601	0.422586	PROM1/RPGRIP1L	2
BP	GO:0060350	endochondral bone morphogenesis	2/77	57/18800	0.022853	0.437601	0.422586	MMP13/TRPV4	2
BP	GO:0006631	fatty acid metabolic process	5/77	395/18800	0.02299	0.437601	0.422586	GSTA1/SLC27A2/CROT/PIBF1/DAGLB	5
BP	GO:0050891	multicellular organismal water homeostasis	2/77	59/18800	0.024371	0.437601	0.422586	TP63/TRPV4	2
BP	GO:0030865	cortical cytoskeleton organization	2/77	61/18800	0.02593	0.437601	0.422586	TRPV4/FHOD3	2
BP	GO:0046530	photoreceptor cell differentiation	2/77	62/18800	0.026725	0.437601	0.422586	PROM1/RPGRIP1L	2
BP	GO:1905515	non-motile cilium assembly	2/77	63/18800	0.027529	0.437601	0.422586	PIBF1/RPGRIP1L	2
BP	GO:0098742	cell-cell adhesion via plasma-membrane adhesion molecules	4/77	279/18800	0.027617	0.437601	0.422586	DSG3/DSC3/CDH26/IGSF9	4
BP	GO:0034329	cell junction assembly	5/77	420/18800	0.028948	0.437601	0.422586	DNER/COL17A1/DST/TRPV4/SIX4	5
BP	GO:0006749	glutathione metabolic process	2/77	65/18800	0.029166	0.437601	0.422586	GSTA1/GSTA2	2
BP	GO:0030104	water homeostasis	2/77	66/18800	0.029999	0.437601	0.422586	TP63/TRPV4	2
BP	GO:0030239	myofibril assembly	2/77	66/18800	0.029999	0.437601	0.422586	SIX4/FHOD3	2
BP	GO:0055002	striated muscle cell development	2/77	67/18800	0.030841	0.437601	0.422586	SIX4/FHOD3	2
BP	GO:0071466	cellular response to xenobiotic stimulus	3/77	168/18800	0.031689	0.437601	0.422586	GSTA1/ALDH3A1/GSTA2	3
BP	GO:0045109	intermediate filament organization	2/77	68/18800	0.031693	0.437601	0.422586	KRT5/KRT15	2
BP	GO:0003407	neural retina development	2/77	70/18800	0.033424	0.437601	0.422586	PROM1/RPGRIP1L	2
BP	GO:1904888	cranial skeletal system development	2/77	70/18800	0.033424	0.437601	0.422586	TP63/SIX4	2
BP	GO:0001736	establishment of planar polarity	2/77	72/18800	0.035192	0.437601	0.422586	TP63/RPGRIP1L	2
BP	GO:0007164	establishment of tissue polarity	2/77	72/18800	0.035192	0.437601	0.422586	TP63/RPGRIP1L	2
BP	GO:0001822	kidney development	4/77	303/18800	0.035793	0.437601	0.422586	PROM1/HSPB11/RPGRIP1L/SIX4	4
BP	GO:0061512	protein localization to cilium	2/77	75/18800	0.037909	0.437601	0.422586	WDR35/DZIP1L	2
BP	GO:0006635	fatty acid beta-oxidation	2/77	76/18800	0.038833	0.437601	0.422586	SLC27A2/CROT	2
BP	GO:0072001	renal system development	4/77	312/18800	0.039185	0.437601	0.422586	PROM1/HSPB11/RPGRIP1L/SIX4	4
BP	GO:0055001	muscle cell development	3/77	183/18800	0.039289	0.437601	0.422586	DNER/SIX4/FHOD3	3
BP	GO:0033504	floor plate development	1/77	10/18800	0.04022	0.437601	0.422586	DZIP1L	1
BP	GO:0043587	tongue morphogenesis	1/77	10/18800	0.04022	0.437601	0.422586	SIX4	1
BP	GO:0060742	epithelial cell differentiation involved in prostate gland development	1/77	10/18800	0.04022	0.437601	0.422586	TP63	1
BP	GO:0098917	retrograde trans-synaptic signaling	1/77	10/18800	0.04022	0.437601	0.422586	DAGLB	1
BP	GO:1902459	positive regulation of stem cell population maintenance	1/77	10/18800	0.04022	0.437601	0.422586	TP63	1
BP	GO:1904672	regulation of somatic stem cell population maintenance	1/77	10/18800	0.04022	0.437601	0.422586	TP63	1
BP	GO:0007492	endoderm development	2/77	78/18800	0.040705	0.437601	0.422586	SOX2/PAX9	2
BP	GO:0007389	pattern specification process	5/77	463/18800	0.041325	0.437601	0.422586	TP63/DZIP1L/HSPB11/BBS5/RPGRIP1L	5
BP	GO:0060249	anatomical structure homeostasis	4/77	319/18800	0.041946	0.437601	0.422586	NELL2/PROM1/PIP/MUC4	4
BP	GO:0006575	cellular modified amino acid metabolic process	3/77	188/18800	0.042011	0.437601	0.422586	GSTA1/CROT/GSTA2	3
BP	GO:1902806	regulation of cell cycle G1/S phase transition	3/77	188/18800	0.042011	0.437601	0.422586	MNAT1/MLF1/SOX2	3
BP	GO:0001895	retina homeostasis	2/77	80/18800	0.042611	0.437601	0.422586	PROM1/PIP	2
BP	GO:0002924	negative regulation of humoral immune response mediated by circulating immunoglobulin	1/77	11/18800	0.044153	0.437601	0.422586	SUSD4	1
BP	GO:0039532	negative regulation of viral-induced cytoplasmic pattern recognition receptor signaling pathway	1/77	11/18800	0.044153	0.437601	0.422586	TSPAN6	1
BP	GO:0043589	skin morphogenesis	1/77	11/18800	0.044153	0.437601	0.422586	TP63	1
BP	GO:0046598	positive regulation of viral entry into host cell	1/77	11/18800	0.044153	0.437601	0.422586	TMPRSS4	1
BP	GO:0060221	retinal rod cell differentiation	1/77	11/18800	0.044153	0.437601	0.422586	RPGRIP1L	1
BP	GO:0060601	lateral sprouting from an epithelium	1/77	11/18800	0.044153	0.437601	0.422586	TP63	1
BP	GO:0070944	neutrophil-mediated killing of bacterium	1/77	11/18800	0.044153	0.437601	0.422586	CXCL6	1
BP	GO:0071472	cellular response to salt stress	1/77	11/18800	0.044153	0.437601	0.422586	TRPV4	1
BP	GO:0071609	chemokine (C-C motif) ligand 5 production	1/77	11/18800	0.044153	0.437601	0.422586	TRPV4	1
BP	GO:0071649	regulation of chemokine (C-C motif) ligand 5 production	1/77	11/18800	0.044153	0.437601	0.422586	TRPV4	1
BP	GO:0072584	caveolin-mediated endocytosis	1/77	11/18800	0.044153	0.437601	0.422586	PROM2	1
BP	GO:0075294	positive regulation by symbiont of entry into host	1/77	11/18800	0.044153	0.437601	0.422586	TMPRSS4	1
BP	GO:0048839	inner ear development	3/77	192/18800	0.044256	0.437601	0.422586	SOX2/RPGRIP1L/SIX4	3
BP	GO:0002024	diet induced thermogenesis	1/77	12/18800	0.048071	0.437601	0.422586	TRPV4	1
BP	GO:0007501	mesodermal cell fate specification	1/77	12/18800	0.048071	0.437601	0.422586	EYA2	1
BP	GO:0021670	lateral ventricle development	1/77	12/18800	0.048071	0.437601	0.422586	RPGRIP1L	1
BP	GO:0021781	glial cell fate commitment	1/77	12/18800	0.048071	0.437601	0.422586	SOX2	1
BP	GO:0033540	fatty acid beta-oxidation using acyl-CoA oxidase	1/77	12/18800	0.048071	0.437601	0.422586	CROT	1
BP	GO:0035112	genitalia morphogenesis	1/77	12/18800	0.048071	0.437601	0.422586	TP63	1
BP	GO:0045916	negative regulation of complement activation	1/77	12/18800	0.048071	0.437601	0.422586	SUSD4	1
BP	GO:0048548	regulation of pinocytosis	1/77	12/18800	0.048071	0.437601	0.422586	PROM2	1
BP	GO:0051095	regulation of helicase activity	1/77	12/18800	0.048071	0.437601	0.422586	MNAT1	1
BP	GO:0051639	actin filament network formation	1/77	12/18800	0.048071	0.437601	0.422586	FHOD3	1
BP	GO:0060788	ectodermal placode formation	1/77	12/18800	0.048071	0.437601	0.422586	SIX4	1
BP	GO:0070943	neutrophil-mediated killing of symbiont cell	1/77	12/18800	0.048071	0.437601	0.422586	CXCL6	1
BP	GO:0071697	ectodermal placode morphogenesis	1/77	12/18800	0.048071	0.437601	0.422586	SIX4	1
BP	GO:0072182	regulation of nephron tubule epithelial cell differentiation	1/77	12/18800	0.048071	0.437601	0.422586	PROM1	1
BP	GO:0072497	mesenchymal stem cell differentiation	1/77	12/18800	0.048071	0.437601	0.422586	SLC4A11	1
BP	GO:0030433	ubiquitin-dependent ERAD pathway	2/77	86/18800	0.048523	0.437601	0.422586	CLGN/UBXN10	2
CC	GO:0036064	ciliary basal body	6/80	161/19594	5.10E-05	0.007803	0.007194	WDR35/DZIP1L/MLF1/EFHC2/BBS5/RPGRIP1L	6
CC	GO:0005930	axoneme	5/80	131/19594	0.000199	0.01052	0.009698	WDR35/DZIP1L/EFHC2/BBS5/RPGRIP1L	5
CC	GO:0097014	ciliary plasm	5/80	132/19594	0.000206	0.01052	0.009698	WDR35/DZIP1L/EFHC2/BBS5/RPGRIP1L	5
CC	GO:0032838	plasma membrane bounded cell projection cytoplasm	6/80	220/19594	0.000282	0.010769	0.009928	WDR35/DZIP1L/DST/EFHC2/BBS5/RPGRIP1L	6
CC	GO:0099568	cytoplasmic region	6/80	259/19594	0.000668	0.020441	0.018845	WDR35/DZIP1L/DST/EFHC2/BBS5/RPGRIP1L	6
CC	GO:0005788	endoplasmic reticulum lumen	6/80	311/19594	0.001711	0.043624	0.040218	SLC27A2/GOLM1/TOR4A/CP/COL17A1/P3H2	6
CC	GO:0060170	ciliary membrane	3/80	75/19594	0.003583	0.076818	0.070819	PROM2/PROM1/BBS5	3
CC	GO:0030990	intraciliary transport particle	2/80	24/19594	0.004286	0.076818	0.070819	WDR35/HSPB11	2
CC	GO:0030057	desmosome	2/80	25/19594	0.004647	0.076818	0.070819	DSG3/DSC3	2
CC	GO:0031528	microvillus membrane	2/80	26/19594	0.005021	0.076818	0.070819	PROM2/PROM1	2
CC	GO:0005604	basement membrane	3/80	95/19594	0.006928	0.096362	0.088837	COL17A1/DST/P3H2	3
CC	GO:0001533	cornified envelope	2/80	45/19594	0.014548	0.174943	0.161282	DSG3/DSC3	2
CC	GO:0097542	ciliary tip	2/80	47/19594	0.015802	0.174943	0.161282	WDR35/HSPB11	2
CC	GO:0005911	cell-cell junction	6/80	497/19594	0.016008	0.174943	0.161282	DSG3/TRIM29/DSC3/COL17A1/TRPV4/RPGRIP1L	6
CC	GO:0045177	apical part of cell	5/80	424/19594	0.029701	0.302951	0.279294	PROM2/SLC4A11/CHL1/PROM1/TRPV4	5
CC	GO:0005881	cytoplasmic microtubule	2/80	75/19594	0.037706	0.337417	0.311069	TRPV4/RPGRIP1L	2
CC	GO:0019908	nuclear cyclin-dependent protein kinase holoenzyme complex	1/80	10/19594	0.040096	0.337417	0.311069	MNAT1	1
CC	GO:0035253	ciliary rootlet	1/80	11/19594	0.044017	0.337417	0.311069	RPGRIP1L	1
CC	GO:0000439	transcription factor TFIIH core complex	1/80	12/19594	0.047922	0.337417	0.311069	MNAT1	1
MF	GO:0004364	glutathione transferase activity	2/81	26/18410	0.005803	0.34647	0.332992	GSTA1/GSTA2	2
MF	GO:0043014	alpha-tubulin binding	2/81	39/18410	0.012751	0.34647	0.332992	TRPV4/EFHC2	2
MF	GO:0015485	cholesterol binding	2/81	50/18410	0.020434	0.34647	0.332992	PROM2/PROM1	2
MF	GO:0098632	cell-cell adhesion mediator activity	2/81	54/18410	0.023603	0.34647	0.332992	TRIM29/IGSF9	2
MF	GO:0005080	protein kinase C binding	2/81	55/18410	0.024424	0.34647	0.332992	NELL2/TRPV4	2
MF	GO:0016765	transferase activity, transferring alkyl or aryl (other than methyl) groups	2/81	59/18410	0.027826	0.34647	0.332992	GSTA1/GSTA2	2
MF	GO:0032934	sterol binding	2/81	60/18410	0.028705	0.34647	0.332992	PROM2/PROM1	2
MF	GO:0005178	integrin binding	3/81	156/18410	0.0315	0.34647	0.332992	PTPRZ1/CDH26/DST	3
MF	GO:0098631	cell adhesion mediator activity	2/81	64/18410	0.032329	0.34647	0.332992	TRIM29/IGSF9	2
MF	GO:0002039	p53 binding	2/81	66/18410	0.034205	0.34647	0.332992	TRIM29/TP63	2
MF	GO:0097110	scaffold protein binding	2/81	67/18410	0.035159	0.34647	0.332992	KRT5/KRT15	2
MF	GO:0004252	serine-type endopeptidase activity	3/81	174/18410	0.04143	0.34647	0.332992	TMPRSS4/MMP13/RHBDL2	3
MF	GO:0015245	fatty acid transmembrane transporter activity	1/81	10/18410	0.043147	0.34647	0.332992	SLC27A2	1
MF	GO:0031957	very long-chain fatty acid-CoA ligase activity	1/81	10/18410	0.043147	0.34647	0.332992	SLC27A2	1
MF	GO:0036312	phosphatidylinositol 3-kinase regulatory subunit binding	1/81	10/18410	0.043147	0.34647	0.332992	FAM83B	1
MF	GO:0045294	alpha-catenin binding	1/81	10/18410	0.043147	0.34647	0.332992	CDH26	1
MF	GO:0003779	actin binding	5/81	439/18410	0.044213	0.34647	0.332992	TNS4/DST/PIP/TRPV4/FHOD3	5
MF	GO:0019864	IgG binding	1/81	11/18410	0.047359	0.34647	0.332992	PIP	1
MF	GO:0047676	arachidonate-CoA ligase activity	1/81	11/18410	0.047359	0.34647	0.332992	SLC27A2	1
MF	GO:0097371	MDM2/MDM4 family protein binding	1/81	11/18410	0.047359	0.34647	0.332992	TP63	1

GO, Gene Ontology; BP, biological process; CC, cellular component; MF, molecular function; ERAD, ER-associated ubiquitin-dependent protein breakdown; TFIIH, transcription factor IIH.

Table S3 KEGG analysis of blue module genes

ID	Description	Gene Ratio	BgRatio	p value	p.adjust	q value	Gene ID	Count
hsa05418	Fluid shear stress and atherosclerosis	4/30	139/8159	0.00156715	0.08974693	0.08054849	CALML4/GSTA1/TRPV4/GSTA2	4
hsa00982	Drug metabolism - cytochrome P450	3/30	72/8159	0.00225502	0.08974693	0.08054849	GSTA1/ALDH3A1/GSTA2	3
hsa00980	Metabolism of xenobiotics by cytochrome P450	3/30	78/8159	0.00283411	0.08974693	0.08054849	GSTA1/ALDH3A1/GSTA2	3
hsa04657	IL-17 signaling pathway	3/30	94/8159	0.00480009	0.11400204	0.10231762	MMP13/CXCL6/MUC5B	3
hsa00480	Glutathione metabolism	2/30	57/8159	0.01840355	0.31255924	0.28052408	GSTA1/GSTA2	2
hsa05204	Chemical carcinogenesis - DNA adducts	2/30	69/8159	0.0263271	0.31255924	0.28052408	GSTA1/GSTA2	2
hsa01524	Platinum drug resistance	2/30	73/8159	0.02922643	0.31255924	0.28052408	GSTA1/GSTA2	2
hsa05133	Pertussis	2/30	76/8159	0.0314814	0.31255924	0.28052408	CALML4/CXCL6	2
hsa05202	Transcriptional misregulation in cancer	3/30	193/8159	0.03311686	0.31255924	0.28052408	PROM1/MLF1/SIX4	3
hsa00983	Drug metabolism - other enzymes	2/30	80/8159	0.03459216	0.31255924	0.28052408	GSTA1/GSTA2	2
hsa04146	Peroxisome	2/30	82/8159	0.03619107	0.31255924	0.28052408	SLC27A2/CROT	2
hsa04970	Salivary secretion	2/30	92/8159	0.044602	0.33904891	0.30429875	CALML4/MUC5B	2
hsa04750	Inflammatory mediator regulation of TRP channels	2/30	98/8159	0.0499651	0.33904891	0.30429875	CALML4/TRPV4	2
hsa04925	Aldosterone synthesis and secretion	2/30	98/8159	0.0499651	0.33904891	0.30429875	CALML4/DAGLB	2

KEGG, Kyoto Encyclopedia of Genes and Genomes; TRP, transient receptor potential.

https://dx.doi.org/10.21037/atm-22-6161